

Distillation of optical Fock states using atom-cavity systems

G.P. Teja^{1,*} and Chanchal^{2,†}

¹ Nanyang Technological University, 21 Nanyang Link, Singapore 637371, Singapore

² Department of Physical Sciences, Indian Institute of Science Education and Research, Mohali, Punjab, 140306, India



(Received 11 April 2023; revised 16 August 2023; accepted 3 October 2023; published 18 October 2023)

Fock states are quantized states of electromagnetic waves with diverse applications in quantum optics and quantum communication. However, the generation of arbitrary optical Fock states still remains elusive. Most Fock-state-generation proposals rely on precisely controlling the atom-cavity interactions and are experimentally challenging. We propose a scheme to distill an optical Fock state from a coherent state. A conditional phase flip with arbitrary phase is implemented between the atom and light. The conditional phase flip along with unitary rotations and measurements on the atoms enables us to distill the required Fock state. As an example, we show the distillation of Fock state $|100\rangle$.

DOI: 10.1103/PhysRevApplied.20.044049

I. INTRODUCTION

The second quantization of electromagnetic fields reveals the equivalence of light modes with harmonic oscillators [1]. The eigenstates of these oscillators are called the “Fock states” and they describe the number of photons present in a specific mode of a light field. Because of their highly nonclassical nature, they are extremely useful areas such as quantum metrology, quantum key distribution protocols, and quantum computation [2,3]. However, their quantum nature also makes it difficult to produce them. In existing experiments, optical Fock states are produced with use of parametric down-conversion and photon-number detectors. These techniques have been shown to produce Fock states of up to five photons [4–8]; however, it is still a challenging task to produce higher Fock states in the optical regime.

Atom-cavity systems have been widely studied for the deterministic generation of optical Fock states. Fock states are created inside the cavity by controlling the interaction between atoms and the cavity [9–11]. However, this requires precise control that is limited by the coherence time of the system. As the number of photons increases, control becomes harder and the fidelity of the generated Fock states decreases [12], making it difficult to generate high-photon-number states.

In addition to control of the dynamics of atom-cavity systems, schemes based on feedback mechanisms have also been proposed for the deterministic generation of Fock states [13,14]. These schemes involve the use of

a controller to probe the cavity mode with weak measurements, which provide information about the cavity field. On the basis of the information obtained from these measurements, an actuator applies feedback to the cavity. By repeated measurement and application of feedback, the cavity state can be prepared in any desired state. This method has been experimentally verified with use of Rydberg atoms and superconducting cavities [15].

Further, another method for Fock-state sorting has been demonstrated that uses chiral coupling of a qubit to a waveguide. In this method, the light acquires a Fock-number-dependent delay, and the incident pulse is sorted temporally by its Fock numbers [16,17].

In this article, we propose a protocol to distill Fock states from a coherent state. It is based on repeated reflection of light from the atom-cavity system. Unlike existing protocols, this does not require precise control or feedback mechanisms. Also the Fock states in this scheme are generated outside the cavity, avoiding further extraction that can effect the statistics of the light.

In Sec. II we discuss the conditional phase flip (CPF) between the atom and the light mode and study effects of cavity-light detuning on the CPF. In Sec. III the atom-photon phase gate along with unitary rotations and measurements is used to distill a Fock state from a coherent state. Finally, we discuss possible implementations.

II. ATOM-PHOTON GATE

Atom-photon gates aim to create a CPF between an atom and a flying photon. Typically this is confined only to a phase of π as this is sufficient to implement a general unitary operation on atom-photon and photon-photon systems.

*teja4477@gmail.com

†chanchal4592@gmail.com

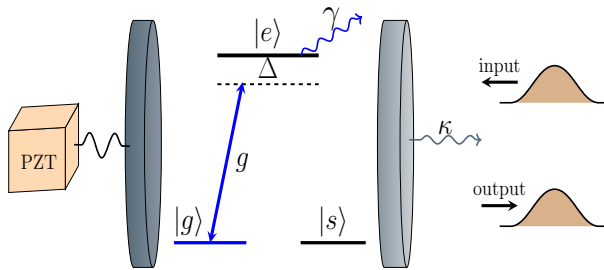


FIG. 1. Atom-cavity system for the CPF. A Λ -type atom with only $|e\rangle \leftrightarrow |g\rangle$ transition interacts with the cavity mode. g and κ are the coupling strength and the cavity decay rate of the cavity mode. Δ is the detuning of the cavity mode with input light and the atom. The second mirror is attached to a piezoelectric actuator (PZT) to tune the cavity resonant frequency.

To obtain a conditional phase shift, we consider a three-level atom with ground states $|g\rangle$ and $|s\rangle$ and an excited state $|e\rangle$ as shown in Fig. 1. Here, only the transition ($|e\rangle \leftrightarrow |g\rangle$) is coupled to the cavity mode. The Hamiltonian of such a system can be written as

$$H = \hbar\omega_c \hat{a}^\dagger \hat{a} + \hbar\omega_{eg} |e\rangle \langle e| + \hbar g (\sigma_{eg} \hat{a} + \sigma_{ge} \hat{a}^\dagger), \quad (1)$$

where ω_{eg} (ω_c) is the transition frequency for the atom (cavity), g is the atom-cavity coupling strength, $\sigma_{eg} = |e\rangle \langle g|$ is the atomic operator, and \hat{a} is the cavity-mode operator. Although we are considering a single three-level atom interacting with the cavity mode, the following results can be extended to dark states in N three-level systems and N atoms under Rydberg-blockade conditions [18,19].

Solving Eq. (1) for the dynamics yields reflection coefficients r_1 and r_0 (see Appendix A for details):

$$r_1 = 1 - \frac{2}{(1 + 4C) - i\Delta}, \quad r_0 = 1 - \frac{2}{1 - i\Delta}, \quad (2)$$

where r_1 is the reflection coefficient for the coupled transition, r_0 is the reflection coefficient for the decoupled transition (empty cavity) [20], $C = g^2/\kappa\gamma$ is the cooperativity, and $\Delta = 2\Delta_c/\kappa$, where $\Delta_c = \omega_c - \omega_L$, with ω_L being the mean frequency of the input pulse. Assuming that $C \gg 1$ gives $r_1 \simeq 1$ and r_0 can be any phase $e^{i\phi}$. For example, numerically solving r_0 for $\phi = \{\pi/2, \pi/4, \pi/8, \pi/16\}$ gives $\Delta = \{-1, -2.4142, -5.0273, -10.1531\}$.

By use of Eq. (2) under strong atom-cavity coupling, the operation for the atom-cavity reflection can be written as (see Appendix A)

$$\hat{D}(\phi) = |g\rangle \langle g| \otimes \mathcal{I} + |s\rangle \langle s| \otimes \exp\{i\phi \hat{n}\}. \quad (3)$$

Note that cavity-light resonance $\Delta = 0$ gives $r_0 = -1$ [$\hat{D}(\pi)$]. This resonance condition has been exploited to generate atom-photon gates between atoms and a single

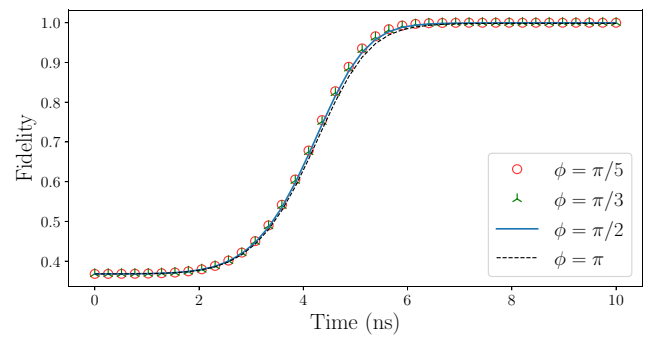


FIG. 2. $\hat{D}(\phi)$ operation attained from the steady-state dynamics of the atom-cavity system. We set $g = 2\pi \times 16$ GHz, $\kappa = 2\pi \times 5$ GHz, and $\gamma = 2\pi \times 0.05$ GHz for the numerical simulations.

photon [21]. Further, Eq. (3) transforms a coherent state into

$$\hat{D}(\pi)[\psi_a \otimes |\alpha\rangle] = \frac{1}{\sqrt{2}}(|g\rangle |\alpha\rangle + |s\rangle |-\alpha\rangle), \quad (4)$$

where $\psi_a = \frac{1}{\sqrt{2}}(|g\rangle + |s\rangle)$. Performing a $\pi/2$ rotation and a measurement on the atom projects the light to a cat state. This has been experimentally verified by trapping ^{87}Rb to generate cat states with strength $\alpha = 1.4$ [22].

The reflection coefficients are derived under the assumption that the atom-cavity system quickly attains a steady state. Although this is true on resonance [23], detuning can effect the dynamics. To verify that steady states are attained even with detuning, we use input-output theory with quantum pulses to solve for the complete dynamics [23,24]. On reflection of light from the atom-cavity system, the transformation

$$\psi_a |\psi\rangle_{\text{in}} |0\rangle_{\text{out}} \xrightarrow{\text{reflection}} |0\rangle_{\text{in}} \frac{|g\rangle |\psi\rangle_{\text{out}} + |s\rangle e^{i\phi \hat{n}} |\psi\rangle_{\text{out}}}{\sqrt{2}} \quad (5)$$

is expected, and $|\psi\rangle_{\text{in}} = \sum_n C_n |n\rangle$ and $|\psi\rangle_{\text{out}} = \sum_n C_n |n\rangle$ represent the quantum states of the input and output light modes.

In Fig. 2 we plot the fidelity for various phases. Here, input light is reflected from the atom-cavity system and the quantum state of the atom and the output light is numerically obtained. Then the fidelity is evaluated between the obtained output state and the expected output state [Eq. (5)] (see Appendix B for more details). From the plot it is clear that reflection from the atom-cavity system yields the operation $\hat{D}(\phi)$ on the output light mode and a steady state is obtained even in the presence of cavity-light detuning.

III. DISTILLATION OF FOCK STATES

We now use the phase-shift operation $\hat{D}(\phi)$, local unitary, and measurement on an atom to distill a Fock state. The protocol consists of the following steps:

- (1) To prepare the Fock state $|\mathcal{A}\rangle$, we start with a coherent state of amplitude $\alpha = \sqrt{\mathcal{A}}$.
- (2) The atom is prepared in the state $\psi_a = \frac{1}{\sqrt{2}}(|g\rangle + |s\rangle)$.
- (3) The light is reflected from the atom-cavity setup to perform $\hat{D}(\phi)$.
- (4) A unitary rotation U_a is performed on the atom. The unitary rotation can be executed by stimulated Raman adiabatic passage with errors below 10^{-4} [25].
- (5) A measurement is performed on the atom [22].

The choice of $\alpha = \sqrt{\mathcal{A}}$ is not a stringent condition; rather this choice is based on the fact that a coherent state has a Poisson distribution with a peak value at α^2 . The state of the “atom plus output light” after step 3 can be written as

$$\Psi = \frac{1}{\sqrt{2}} [\psi_l |g\rangle + \exp\{i\phi\hat{n}\} \psi_l |s\rangle], \quad (6)$$

where $\psi_l = \sum_n C_n |n\rangle$ is the state of light. By application of an appropriate $U_a[\theta]$, the atom-cavity state can always be cast in the form

$$\Psi = \sum_k C_k |k\rangle |g\rangle + \sum_l C_l |l\rangle |s\rangle, \quad (7)$$

where $k \neq l$ and $\sum_k |C_k|^2 + \sum_l |C_l|^2 = 1$, and measurement on the atom gives the photonic state

$$\psi_l = \sum_k C_k |k\rangle \quad \text{or} \quad \psi_l = \sum_l C_l |l\rangle, \quad (8)$$

where $\sum_k |C_k|^2$ and $\sum_l |C_l|^2$ are the probabilities for the atomic measurements $|g\rangle$ and $|s\rangle$.

By repeating steps 2–5, one can distill a general Fock state. We establish this by explicitly showing the distillation of the Fock state $|100\rangle$. The atom is initialized in the state ψ_a and the input light is in the coherent state $|\alpha = 10\rangle$. The initial state of atom and light can be written as (see Appendix C)

$$\Psi = \sum_{k=70}^{130} C_k |k\rangle \otimes \frac{1}{\sqrt{2}}(|g\rangle + |s\rangle), \quad (9)$$

where the coherent state is approximated as $|\alpha = 10\rangle \simeq \sum_{k=70}^{130} C_k |k\rangle$. The explicit form C_k is irrelevant to the

distillation protocol and is used only to calculate measurement probabilities. Performing $\hat{D}(\pi)$ on Ψ yields

$$\Psi_\pi = \sum_{k=70}^{130} C_k e^{i\pi\hat{n}} |k\rangle |s\rangle + \sum_{n=70}^{130} C_k |k\rangle |g\rangle, \quad (10)$$

where Ψ_l represents the state of output light after application of the operation $\hat{D}(l)$. Note that $\hat{D}(\pi)$ is obtained on resonance, i.e., $\Delta = 0$. Performing the atomic unitary $U_a[0]$ and measuring the atom in the state $|g\rangle$ removes the odd photons to give the even cat state [22]

$$\Psi_\pi = \sum_{k=36}^{64} C_{2k} |2k\rangle, \quad (11)$$

where the normalization is absorbed into C_{2k} , i.e., $\sum_{k=36}^{64} |C_{2k}|^2 = 1$.

Preparing the atom in ψ_a and reflecting the state Ψ_π with $\hat{D}(\pi/2)$ yields

$$\Psi_{\frac{\pi}{2}} = \sum_{k=36}^{64} C_{2k} [(-1)^k |s\rangle + |g\rangle] |2k\rangle. \quad (12)$$

Performing $U_a[0]$ and a measurement in $|g\rangle$ projects the photonic state to $\Psi_{\pi/2} = \sum_{k=18}^{32} C_{4k} |4k\rangle$. Reflecting the state $\Psi_{\pi/2}$ with $\hat{D}(\pi/4)$ yields

$$\Psi_{\frac{\pi}{4}} = \sum_{k=18}^{32} C_{4k} [(-1)^k |s\rangle + |g\rangle] |4k\rangle. \quad (13)$$

Applying $U_a[0]$ and a measurement in $|s\rangle$ projects the light state to $\Psi_{\pi/4} = \sum_{k=9}^{15} C_{8k+4} |8k+4\rangle$. Reflecting $\Psi_{\pi/4}$ with $\hat{D}(\pi/8)$ yields

$$\Psi_{\frac{\pi}{8}} = \sum_{k=9}^{15} C_{8k+4} [(-1)^k e^{i\pi/2} |s\rangle + |g\rangle] |8k+4\rangle. \quad (14)$$

To cancel the extra factor of $\pi/2$, we perform $U_a[\pi/2]$. Measuring the atom in $|g\rangle$ projects the light state to

$$\begin{aligned} \Psi_{\frac{\pi}{8}} &= \sum_{k=5}^7 C_{16k+4} |16k+4\rangle, \\ &= C_{84} |84\rangle + C_{100} |100\rangle + C_{116} |116\rangle. \end{aligned} \quad (15)$$

Again reflecting $\Psi_{\pi/8}$ with $\hat{D}(\pi/16)$ gives

$$\Psi_{\frac{\pi}{16}} = \sum_{k=5}^7 C_{16k+4} [(-1)^k e^{\frac{i\pi}{4}} |s\rangle + |g\rangle] |16k+4\rangle, \quad (16)$$

and finally performing $U_a[\pi/4]$ and measurement in $|s\rangle$ distills the Fock state $|100\rangle$.

TABLE I. Distillation of Fock states. First column shows the sequence of distilled Fock numbers after each iteration. Second column shows the atom-cavity phase, $\hat{D}(\phi)$. Other columns show the unitary operation $U_a[\theta]$ and the measurement (\mathcal{M}) on the atom. \mathcal{P} is the probability of the outcome after each iteration. Note that atom is prepared in $|\psi_a\rangle$ after each iteration.

Distilled Fock nos.		ϕ	θ	\mathcal{M}	\mathcal{P}
$(k)_{k=70}^{130}$	70, 71, ..., 100, ..., 129, 130	π	0	$ g\rangle$	
$(2k)_{k=36}^{64}$	70, 72, ..., 100, ..., 126, 128	$\pi/2$	0	$ g\rangle$	0.5
$(4k)_{k=18}^{32}$	72, 76, ..., 100, ..., 124, 128	$\pi/4$	0	$ s\rangle$	0.5
$(8k+4)_{k=9}^{15}$	76, 84, ..., 100, ..., 116, 124	$\pi/8$	$\pi/2$	$ g\rangle$	0.5
$(16k+4)_{k=5}^7$	84, 100, 116	$\pi/16$	$\pi/4$	$ g\rangle$	0.5
$(16k+4)_{k=6}$	100	0.64

The distillation protocol discussed above is summarized in Table I, and it is clear that an arbitrary Fock state can be distilled by multiple iterations. We started with a coherent state with mean and variance of $|\alpha|^2$. For high \mathcal{A} , the probability distribution can be approximated with a Gaussian, and $\pm 3\sqrt{\mathcal{A}}$ covers 0.997 of the total area of a Gaussian distribution (see Appendix C). Also from Table I, we notice that in each iteration, the total Fock numbers reduce by half. Thus, the total number of iterations (\mathcal{Q}) required to distill a Fock state from the coherent state can be written as

$$6\sqrt{\mathcal{A}} = 2^{\mathcal{Q}+1} \Rightarrow \mathcal{Q} = \lceil \log_2(6(\Delta\hat{n})) \rceil - 1, \quad (17)$$

where $\lceil \cdot \rceil$ is the ceiling function and $\langle \Delta\hat{n} \rangle = [\langle \hat{n}^2 \rangle - \langle \hat{n} \rangle^2]^{1/2}$ is the standard deviation of the coherent state. Although Eq. (17) is obtained by our assuming high coherent-state amplitude, it works even for small amplitudes. Further, squeezed coherent states (SCSs) with optimized squeezing [26] can be used to reduce the numbers of iterations to $\mathcal{Q} - 1$ (see Appendix C).

It is also interesting to note that a general CPF is not required and that phase shifts of the form $\phi = \pi/2^n$ are sufficient for the distillation protocol. Since every iteration requires an atomic measurement, the total probability of success is given by $\mathcal{P} \sim 1/2^{\mathcal{Q}}$. For instance, with $|100\rangle$, we obtain $\mathcal{P} \sim 1/32$ without squeezing and $\mathcal{P} \sim 1/16$ with squeezing. Despite this low probability, each iteration guarantees a nonclassical state, and we can proceed with iterations regardless of measurements, ultimately obtaining a Fock state in the range $[\mathcal{A} - 3\sqrt{\mathcal{A}}, \mathcal{A} + 3\sqrt{\mathcal{A}}]$. For example, through distillation with $|\sqrt{100}\rangle$, we achieve a Fock state between $|70\rangle$ and $|130\rangle$ with unit probability.

Another special case of the distillation protocol is the deletion of prime-numbered Fock states. Prime numbers, by definition, cannot be factored by any other number, and this can be exploited to delete a Fock number from a given state. For example, reflecting the coherent state Ψ [Eq. (9)] with phase $\hat{D}(\pi/101)$, performing $U_a[0]$, and measuring the atom in $|g\rangle$ gives the photonic state $\Psi = \sum_{n=70}^{100} C_n |n\rangle + \sum_{n=102}^{130} C_n |n\rangle$.

IV. IMPLEMENTATIONS AND DISCUSSION

Atom-cavity systems are used to implement a variety of protocols [21]. To implement this protocol, the cavity resonant frequency can be tuned to adjust the detuning Δ . This can be achieved by attaching the cavity mirror to a piezoelectric actuator [27]. Besides tuning of the cavity frequency, multiple atom-cavity systems with different detunings can also be considered. Waveguide QED is an effective approach to study such systems, where an array of atoms are trapped above waveguides or embedded in photonic crystal waveguides to realize many atom-cavity systems on a single chip [28,29]. Overall, the distillation protocol can be verified with use of existing experimental techniques [22,29]. However, in practice, there is a slight probability of photon loss due to unwanted scattering. The scattering losses depend on the properties of the noisy channel and loss-correction techniques. Further, the amount of nonclassicality of the output light increases after each iteration, which in turn can make the quantum states strongly susceptible to transmission and photon losses [30]. The effects of noise, loss corrections, and nonclassicality are intertwined and are beyond the scope of this article. We intend to study them separately.

Also, the coherent state used in the distillation protocol typically has a narrow temporal width, and this can be used to realize a highly nonclassical bath. When the temporal width of the pulse is much narrower than the cavity linewidth, the pulse can effectively act as a bath for an atom-cavity system. This means that the first Markov approximation, which assumes that the system-reservoir coupling strength is frequency independent [31], is satisfied.

Recently we became aware of study similar to ours that also involves sequential application of controlled operation, unitary rotation, and a measurement on the qubit [32]. However, there are notable differences. That study used a two-level system sensitive to decoherence, while we use a stabler Λ -type system with a qubit based on two ground states, differing from the ground-state-and-excited-state approach used in the other study.

Our proposal operates in the optical regime in atom-cavity setups, while the proposal in Ref. [32] focuses on

the microwave regime in a superconducting platform. As a result, the modeling is different. For example, we use a Hamiltonian of the form $\sigma_+ \hat{a} + \sigma_- \hat{a}^\dagger$, while in Ref. [32] a Hamiltonian of the form $\sigma_z \hat{a}^\dagger \hat{a}$ is used.

In the superconducting platform, the Hamiltonian is evolved to obtain the Fock states as standing waves inside a cavity, and the fidelity of these states is reduced by the decay rate of the cavity, which is proportional to the Fock state $|n\rangle$ [32]. In contrast, in our proposal, Fock states are formed outside the cavity as traveling pulses, hence making it robust with regard to cavity decay rates.

ACKNOWLEDGMENTS

We thank Dr. Sandeep K. Goyal and Dr. G. Krishna Teja for their helpful discussions. Chanchal acknowledges the Council of Scientific and Industrial Research, Government of India, for financial support through a research fellowship [Award No. 09/947(0106)/2019-EMR-I].

APPENDIX A: REFLECTION COEFFICIENTS FOR THE ATOM-CAVITY SYSTEM

Here we derive the reflection coefficients introduced in the main text. To understand the reflection coefficients we start with an initial state

$$\Psi_{\text{in}} = (c_g |g\rangle + c_s |s\rangle) \otimes \sum_n c_n \frac{(\hat{a}_{\text{in}}^\dagger)^n}{\sqrt{n!}} |0\rangle, \quad (\text{A1})$$

where $|c_g|^2 + |c_s|^2 = 1$ and $|c_n|^2 = 1$. On reflection, the state is transformed as follows:

$$\begin{aligned} \Psi_{\text{out}} &= (c_g |g\rangle \sum_n c_n \frac{(r_1 \hat{a}_{\text{out}}^\dagger)^n}{\sqrt{n!}} + c_s |s\rangle \sum_n c_n \frac{(r_0 \hat{a}_{\text{out}}^\dagger)^n}{\sqrt{n!}}) |0\rangle \\ &= c_g |g\rangle (r_1)^\hat{n} \sum_n c_n |n\rangle + c_s |s\rangle (r_0)^\hat{n} \sum_n c_n |n\rangle, \end{aligned} \quad (\text{A2})$$

where r_1 is the reflection coefficient for the transition $|e\rangle \leftrightarrow |g\rangle$ and r_0 is the reflection coefficient for the transition $|e\rangle \leftrightarrow |s\rangle$. To explicitly derive the reflection coefficients, we begin with the Hamiltonian of an atom-cavity system:

$$H = \hbar\omega_c \hat{a}^\dagger \hat{a} + \hbar\omega_a |e\rangle \langle e| + \hbar g(\sigma_{eg} \hat{a} + \sigma_{ge} \hat{a}^\dagger). \quad (\text{A3})$$

The dynamics of the system are governed by the time-reversal Langevin equations and the input-output

relation [20]

$$\begin{aligned} \frac{d\hat{x}}{dt} &= -i[\hat{x}H] + \frac{\gamma}{2} [\hat{x}\sigma_{eg}] \sigma_{ge} - \frac{\gamma}{2} \sigma_{eg} [\hat{x}\sigma_{ge}] \\ &\quad - [\hat{x}\hat{a}^\dagger] \left(-\frac{\kappa}{2} \hat{a} + \sqrt{\kappa} \hat{a}_{\text{out}} \right) + \left(-\frac{\kappa}{2} \hat{a}^\dagger + \sqrt{\kappa} \hat{a}_{\text{out}}^\dagger \right) [\hat{x}\hat{a}], \end{aligned} \quad (\text{A4})$$

where \hat{x} is any operator of the atom-cavity system, and γ and κ are the decay rates of the atom and the cavity. Note that the noise terms for atomic decay are omitted because ω_{eg} is in the optical regime, and hence the noise can be assumed to be vacuum noise. The dynamical equations are obtained as

$$\frac{d\hat{a}}{dt} = -i\omega_c \hat{a} - ig\sigma_{ge} - \sqrt{\kappa} \hat{a}_{\text{out}} + \frac{\kappa}{2} \hat{a}, \quad (\text{A5})$$

$$\frac{d\sigma_{ge}}{dt} = -i\omega_a \sigma_{ge} - ig(\sigma_{gg} - \sigma_{ee}) \hat{a} + \frac{\gamma}{2} \sigma_{ge}. \quad (\text{A6})$$

The transformation $[\hat{a}, \sigma_{ge}, \hat{a}_{\text{out}}] \rightarrow [\hat{a}, \sigma_{ge}, \hat{a}_{\text{out}}] e^{-i\omega_L t}$ gives

$$\frac{d\hat{a}}{dt} = -i\Delta_c \hat{a} - ig\sigma_{ge} - \sqrt{\kappa} \hat{a}_{\text{out}} + \frac{\kappa}{2} \hat{a}, \quad (\text{A7})$$

$$\frac{d\sigma_{ge}}{dt} = -i\Delta_a \sigma_{ge} - ig(\sigma_{gg} - \sigma_{ee}) \hat{a} + \frac{\gamma}{2} \sigma_{ge}, \quad (\text{A8})$$

where $\Delta_c = \omega_c - \omega_L$ and $\Delta_a = \omega_a - \omega_L$. The input light is on resonance with the atomic transition ($\Delta_a = 0$). Also, the atom is assumed to be weakly excited, and hence $\sigma_{gg} = 1$. By setting $\frac{\partial \mathbf{x}}{\partial t} = 0$, we obtain the steady-state solutions as

$$\hat{a} = \frac{-\sqrt{\kappa}}{i\Delta_c - \kappa/2 - \frac{g^2}{\gamma/2}} \hat{a}_{\text{out}}. \quad (\text{A9})$$

Use of the input-output relation $\hat{a}_{\text{out}} - \hat{a}_{\text{in}} = \sqrt{\kappa} \hat{a}$, gives the reflection coefficient for the transition $|e\rangle \leftrightarrow |g\rangle$:

$$r_1 = 1 - \frac{2}{1 + 4C - i\Delta}, \quad (\text{A10})$$

where $\Delta = 2\Delta_c/\kappa$ and the cooperativity $C = g^2/\kappa\gamma$. The reflection coefficient for the noninteracting transition $|e\rangle \leftrightarrow |s\rangle$ is obtained by setting $C = 0$:

$$r_0 = 1 - \frac{2}{1 - i\Delta}. \quad (\text{A11})$$

$r_1 \simeq 1$ and $r_0 = e^{i\phi}$ are the reflection coefficients in the main text; see Table II. By use of Eqs. (A2), (A10), and (A11), the transformation under high cooperativity can be formally written as

$$\hat{\mathcal{D}}(\phi) = |g\rangle \langle g| \otimes \mathcal{I} + |s\rangle \langle s| \otimes (r_0)^\hat{n}. \quad (\text{A12})$$

TABLE II. Numerical solutions for reflection coefficients. Here, the cooperativity $C = 250$. Δ represents the detuning required for $r_0 = e^{i\phi}$. We note that $r_1 \simeq 1$.

Δ	$e^{i\phi}$	r_1
-1	$e^{i\pi/2}$	$0.998 + 2 \times 10^{-6}i$
-2.41421	$e^{i\pi/4}$	$0.998 + 4.8 \times 10^{-6}i$
-5.02734	$e^{i\pi/8}$	$0.998 + 10^{-5}i$
-10.15317	$e^{i\pi/16}$	$0.998 + 2.02 \times 10^{-5}i$
-20.35547	$e^{i\pi/32}$	$0.998 + 4.06 \times 10^{-5}i$

APPENDIX B: VERIFICATION OF THE GENERAL PHASE

Here we discuss the verification of the general phase as described in Eq. (A12). For this, we use the general input-output theory with quantum pulses [23,24]. It is based on a density-matrix formalism where the input and output pulses are replaced by virtual cavities coupled to the quantum system. This formalism explicitly incorporates information about the pulse shapes and quantum states of the input and output field modes. The Hamiltonian governing the dynamics of the virtual cavities and the quantum system is given by

$$\hat{H}_T = \hat{H}_S + \frac{i\hbar}{2} [\sqrt{\kappa} k_u(t) \hat{c}_u^\dagger \hat{a} + \sqrt{\kappa} k_v^*(t) \hat{a}^\dagger \hat{c}_v + k_u(t) k_v^*(t) \hat{c}_u^\dagger \hat{c}_v - h.c.], \quad (B1)$$

where H_S denotes the system Hamiltonian, \hat{a} is the system cavity operator, \hat{c}_u and \hat{c}_v represent the input and output virtual cavity field operators with corresponding complex time-dependent coupling strengths $k_u(t)$ and $k_v(t)$, respectively, and κ denotes the usual decay rate of the system cavity.

The time-dependent coupling strengths in this formalism are selected such that the input virtual cavity releases an input field pulse with a required shape $u(t)$, while the output virtual cavity receives the output field with pulse shape $v(t)$. The coupling strengths of the virtual cavity are related to the pulse shapes by [23,24]

$$k_u(t) = \frac{u^*(t)}{\sqrt{1 - \int_0^t |u'(t)|^2 dt'}}, \quad (B2)$$

$$k_v(t) = \frac{-v^*(t)}{\sqrt{\int_0^t |v'(t)|^2 dt'}}.$$

The dynamics of the system are obtained by solving the following Lindblad master equation:

$$\frac{d\rho_{usv}}{dt} = \frac{1}{i\hbar} [\hat{H}_T \rho_{usv}] + \mathcal{D}[\hat{L}_{\text{eff}}] \rho_{usv}, \quad (B3)$$

where ρ_{usv} is the density matrix of the full system, including the input virtual cavity, the system cavity, and the

output virtual cavity, and $\mathcal{D}[\hat{L}_{\text{eff}}]$ represents the time-dependent Lindblad dissipator with

$$\hat{L}_{\text{eff}}(t) = \sqrt{\kappa} \hat{a} + k_u^*(t) \hat{c}_u + k_v^*(t) \hat{c}_v. \quad (B4)$$

Using this, we can solve the master equation for the full system given in Eq. (B3) to obtain the final state.

We consider the atom-cavity system as described in the main text and numerically solve the corresponding master equation using Eq. (B3) with H_T given by

$$\begin{aligned} \hat{H}_T = & \hbar\omega_c \hat{a}^\dagger \hat{a} + \hbar\omega_a |e\rangle \langle e| + \hbar g (\sigma_{eg} \hat{a} + \sigma_{ge} \hat{a}^\dagger) \\ & + \frac{i\hbar}{2} [\sqrt{\kappa} k_u(t) \hat{c}_u^\dagger \hat{a} + \sqrt{\kappa} k_v^*(t) \hat{a}^\dagger \hat{c}_v \\ & + k_u(t) k_v^*(t) \hat{c}_u^\dagger \hat{c}_v - h.c.]. \end{aligned} \quad (B5)$$

This gives the required state of the output field mode and is used to calculate the fidelity of the output field with respect to the state in Eq. (5).

APPENDIX C: DISTILLATION USING SQUEEZED COHERENT STATES

In the main text, we demonstrated distillation using coherent states. It is evident that the number of iterations depends on the Fock distribution. However, use of SCSs can squeeze the Fock distribution, potentially leading to a reduction in the required number of iterations. Here, we provide two examples using SCSs and compare them with coherent states. These techniques can be applied for a general SCS. First we define the mean and variance of quantum light:

$$\begin{aligned} \langle \hat{a}^\dagger \hat{a} \rangle &= \langle \hat{n} \rangle, \quad \langle (\Delta \hat{n})^2 \rangle \equiv \langle \hat{n}^2 \rangle - \langle \hat{n} \rangle^2, \\ Q &= \frac{\langle (\Delta \hat{n})^2 \rangle - \langle \hat{n} \rangle}{\langle \hat{n} \rangle}, \end{aligned} \quad (C1)$$

TABLE III. Distillation of the Fock states $|51\rangle$ and $|100\rangle$. The first column shows the distilled Fock numbers after each iteration. The second column shows the atom-cavity phase, $\mathcal{D}(\phi)$. The other columns show the unitary operation $U_a[\theta]$ and the measurement (\mathcal{M}) on the atom.

Distilled Fock nos.	ϕ	θ	\mathcal{M}
36, 37, ..., 51, ..., 65, 66	π	0	$ s\rangle$
37, 39, ..., 51, ..., 63, 65	$\pi/2$	$\pi/2$	$ s\rangle$
39, 43, ..., 51, ..., 59, 63	$\pi/4$	$3\pi/4$	$ g\rangle$
43, 51, 59	$\pi/8$	$3\pi/8$	$ g\rangle$
51
85, 86, ..., 100, ..., 114, 115	π	0	$ g\rangle$
86, 88, ..., 100, ..., 112, 114	$\pi/2$	0	$ g\rangle$
88, 92, ..., 100, ..., 108, 118	$\pi/4$	0	$ s\rangle$
92, 100, 108	$\pi/8$	$\pi/2$	$ g\rangle$
100

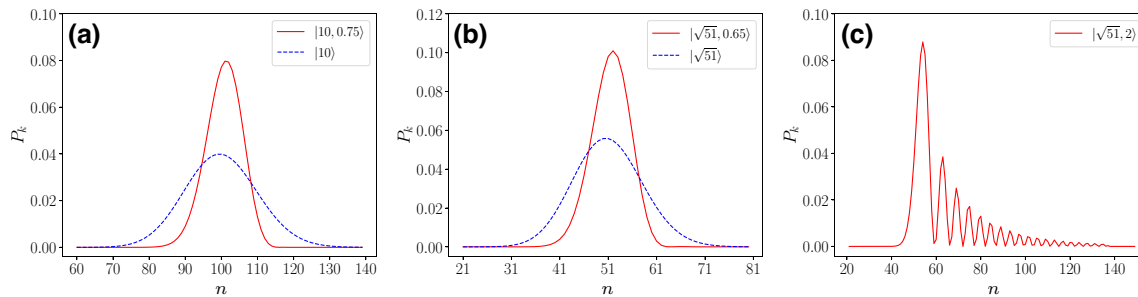


FIG. 3. (a),(b) Number squeezing for the SCS. $|\alpha, r\rangle$ and $|\alpha\rangle$ represent the SCS and the coherent state. An optimal squeezing can result in quantum states that are similar to a coherent state but with reduced variance. Because of the reduced variance, a SCS can be useful in minimizing iterations. (c) The effect of photon-number oscillations for higher squeezing.

When $Q < 0$ ($Q > 0$), the light mode is said to obey sub-Poissonian (super-Poissonian) statistics. The coherent state is written as

$$|\alpha\rangle = e^{-\frac{|\alpha|^2}{2}} \sum_{k=0}^{\infty} \frac{\alpha^k}{\sqrt{k!}} |k\rangle, \quad P_k = e^{-\langle \hat{n} \rangle} \frac{\langle \hat{n} \rangle^k}{k!}, \quad (\text{C2})$$

where $P(k)$ is the probability for the k th Fock state and $\langle \hat{n} \rangle = \langle (\Delta \hat{n})^2 \rangle = |\alpha|^2$. For higher amplitudes, $P(k)$ can be approximated with a Gaussian. Further three standard deviations are expected to include all the statistics:

$$\sum_{n=0}^{\infty} P_k \approx \sum_{\langle \hat{n} \rangle - 3(\Delta \hat{n})}^{\langle \hat{n} \rangle + 3(\Delta \hat{n})} P_k = 0.997. \quad (\text{C3})$$

A general SCS is written as $|\alpha, \xi\rangle = \hat{D}(\alpha') \hat{S}(\xi) |0\rangle$, where $\xi = re^{i\theta}$, $\alpha' = \alpha e^{i\phi}$, and $\phi = \theta/2$, where $\hat{D}(\alpha')$ is the displacement operator and $\hat{S}(r)$ is the squeezing operator. The probability distribution, the variance, and the mean are obtained as [26]

$$P_k^{\text{sq}} = \frac{(\frac{1}{2} \tanh r)^k}{k! \cosh r} e^{-\alpha'^2(1+\tanh r)} \left| H_k \left[\frac{\alpha e^r}{\sqrt{\sinh 2r}} \right] \right|^2, \quad (\text{C4})$$

$$\langle (\Delta \hat{n})^2 \rangle = \alpha'^2 e^{-2r} + 2 \sinh^2 r \cosh^2 r, \quad (\text{C5})$$

$$\langle \hat{n} \rangle = \alpha'^2 + \sinh^2 r, \quad (\text{C6})$$

where $P_k^{\text{sq}} = |\langle n | \alpha', \xi \rangle|^2$ and H_k represents the k th-order Hermite polynomial. With a large coherent contribution ($\alpha \gg \sinh r$) and sub-Poissonian statistics $\langle (\Delta \hat{n})^2 \rangle < \langle \hat{n} \rangle$, a SCS can give rise to the nonclassical effect of number squeezing (see Fig. 3). Similarly to the coherent state [Eq. (C3)] the SCSs $|10, 0.75\rangle$ and $|\sqrt{51}, 0.65\rangle$ are numerically verified to satisfy

$$\sum_{n=0}^{\infty} P_k^{\text{sq}} \approx \sum_{\langle \hat{n} \rangle - 3(\Delta \hat{n})}^{\langle \hat{n} \rangle + 3(\Delta \hat{n})} P_k^{\text{sq}} = 0.9995. \quad (\text{C7})$$

Using Eqs. (17) and (C4), we can determine that four iterations are required to distill Fock states $\{|51\rangle, |100\rangle\}$ from $\{|10, 0.75\rangle, |\sqrt{51}, 0.65\rangle\}$, while use of coherent states $\{|10\rangle, |\sqrt{51}\rangle\}$ requires five iterations. We performed the distillation protocol to verify this; see Table III. Hence, by optimization over the squeezing parameter, we can reduce the number of iterations by 1. However, increasing the squeezing beyond a certain level may cause oscillations in the photon-number distribution and will require more iterations [26]; see Fig. 3.

- [1] R. Loudon *The Quantum Theory of Light*, Oxford Science Publications (Oxford University Press, 2003).
- [2] P. Kok, W. J. Munro, K. Nemoto, T. C. Ralph, J. P. Dowling, and G. J. Milburn, Linear optical quantum computing with photonic qubits, *Rev. Mod. Phys.* **79**, 135 (2007).
- [3] T. Ralph, Quantum optical systems for the implementation of quantum information processing, *Rep. Progr. Phys.* **69**, 853 (2006).
- [4] E. Waks, E. Diamanti, and Y. Yamamoto, Generation of photon number states, *New J. Phys.* **8**, 4 (2006).
- [5] J. Tiedau, T. J. Bartley, G. Harder, A. E. Lita, S. W. Nam, T. Gerrits, and C. Silberhorn, Scalability of parametric down-conversion for generating higher-order Fock states, *Phys. Rev. A* **100**, 041802(R) (2019).
- [6] M. Cooper, L. J. Wright, C. Söller, and B. J. Smith, Experimental generation of multi-photon Fock states, *Opt. Express* **21**, 5309 (2013).
- [7] A. M. Brańczyk, T. Ralph, W. Helwig, and C. Silberhorn, Optimized generation of heralded Fock states using parametric down-conversion, *New J. Phys.* **12**, 063001 (2010).
- [8] A. Lingenfelter, D. Roberts, and A. A. Clerk, Unconditional Fock state generation using arbitrarily weak photonic nonlinearities, *Sci. Adv.* **7**, eabj1916 (2021).
- [9] K. R. Brown, K. M. Dani, D. M. Stamper-Kurn, and K. B. Whaley, Deterministic optical Fock-state generation, *Phys. Rev. A* **67**, 043818 (2003).
- [10] K. Xia, G. K. Brennen, D. Ellinas, and J. Twamley, Deterministic generation of an on-demand Fock state, *Opt. Express* **20**, 27198 (2012).

- [11] C. K. Law and J. H. Eberly, Arbitrary control of a quantum electromagnetic field, *Phys. Rev. Lett.* **76**, 1055 (1996).
- [12] M. Uria, P. Solano, and C. Hermann-Avigliano, Deterministic generation of large Fock states, *Phys. Rev. Lett.* **125**, 093603 (2020).
- [13] I. Dotsenko, M. Mirrahimi, M. Brune, S. Haroche, J.-M. Raimond, and P. Rouchon, Quantum feedback by discrete quantum nondemolition measurements: Towards on-demand generation of photon-number states, *Phys. Rev. A* **80**, 013805 (2009).
- [14] J. M. Geremia, Deterministic and nondestructively verifiable preparation of photon number states, *Phys. Rev. Lett.* **97**, 073601 (2006).
- [15] C. Sayrin, I. Dotsenko, X. Zhou, B. Peaudecerf, T. Rybarczyk, S. Gleyzes, P. Rouchon, M. Mirrahimi, H. Amini, and M. Brune, *et al.*, Real-time quantum feedback prepares and stabilizes photon number states, *Nature* **477**, 73 (2011).
- [16] S. Mahmoodian, G. Calajó, D. E. Chang, K. Hammerer, and A. S. Sørensen, Dynamics of many-body photon bound states in chiral waveguide QED, *Phys. Rev. X* **10**, 031011 (2020).
- [17] F. Yang, M. M. Lund, T. Pohl, P. Lodahl, and K. Mølmer, Deterministic photon sorting in waveguide QED systems, *Phys. Rev. Lett.* **128**, 213603 (2022).
- [18] Y. Sun and P.-X. Chen, Analysis of atom–photon quantum interface with intracavity Rydberg-blocked atomic ensemble via two-photon transition, *Optica* **5**, 1492 (2018).
- [19] Y. Hao, G. Lin, X. Lin, Y. Niu, and S. Gong, Single-photon transistor based on cavity electromagnetically induced transparency with Rydberg atomic ensemble, *Sci. Rep.* **9**, 4723 (2019).
- [20] M. J. Collett and C. W. Gardiner, Squeezing of intracavity and traveling-wave light fields produced in parametric amplification, *Phys. Rev. A* **30**, 1386 (1984).
- [21] A. Reiserer and G. Rempe, Cavity-based quantum networks with single atoms and optical photons, *Rev. Mod. Phys.* **87**, 1379 (2015).
- [22] B. Hacker, S. Welte, S. Daiss, A. Shaukat, S. Ritter, L. Li, and G. Rempe, Deterministic creation of entangled atom–light Schrödinger-cat states, *Nat. Photonics* **13**, 110 (2019).
- [23] A. H. Kiilerich and K. Mølmer, Quantum interactions with pulses of radiation, *Phys. Rev. A* **102**, 023717 (2020).
- [24] A. H. Kiilerich and K. Mølmer, Input-output theory with quantum pulses, *Phys. Rev. Lett.* **123**, 123604 (2019).
- [25] N. V. Vitanov, A. A. Rangelov, B. W. Shore, and K. Bergmann, Stimulated Raman adiabatic passage in physics, chemistry, and beyond, *Rev. Mod. Phys.* **89**, 015006 (2017).
- [26] C. Gerry, P. Knight, and P. L. Knight, *Introductory Quantum Optics* (Cambridge University Press, Cambridge, 2005), Chapter 7.
- [27] K. Möhle, E. V. Kovalchuk, K. Döringshoff, M. Nagel, and A. Peters, Highly stable piezoelectrically tunable optical cavities, *Appl. Phys. B* **111**, 223 (2013).
- [28] D. E. Chang, J. S. Douglas, A. González-Tudela, C.-L. Hung, and H. J. Kimble, Colloquium: Quantum matter built from nanoscopic lattices of atoms and photons, *Rev. Mod. Phys.* **90**, 031002 (2018).
- [29] M. J. R. Staunstrup, A. Tiranov, Y. Wang, S. Scholz, A. D. Wieck, A. Ludwig, L. Midolo, N. Rotenberg, P. Lodahl, and H. L. Jeannic, Direct observation of non-linear optical phase shift induced by a single quantum emitter in a waveguide, [ArXiv:2305.06839](https://arxiv.org/abs/2305.06839) (2023).
- [30] I. L. Chuang, D. W. Leung, and Y. Yamamoto, Bosonic quantum codes for amplitude damping, *Phys. Rev. A* **56**, 1114 (1997).
- [31] C. W. Gardiner and M. J. Collett, Input and output in damped quantum systems: Quantum stochastic differential equations and the master equation, *Phys. Rev. A* **31**, 3761 (1985).
- [32] X. Deng, S. Li, Z.-J. Chen, Z. Ni, Y. Cai, J. Mai, L. Zhang, P. Zheng, H. Yu, C.-L. Zou, S. Liu, F. Yan, Y. Xu, and D. Yu, Heisenberg-limited quantum metrology using 100-photon Fock states, [ArXiv:2306.16919](https://arxiv.org/abs/2306.16919) (2023).